Opto-Electronic Advances

Supplementary information

2022, Vol. 5, No. 10

DOI: 10.29026/oea.2022.210098

Multifunctional flexible optical waveguide sensor: on the bioinspiration for ultrasensitive sensors development

Arnaldo Leal-Junior[1,2], Leticia Avellar[1], Vitorino Biazi[1], M. Simone Soares[3], Anselmo Frizera[1] and Carlos Marques[3]*

[1]Graduate Program in Electrical Engineering, Federal University of Espírito Santo (UFES), Fernando Ferrari Avenue, Vitória 29075-910, Brazil; [2]Mechanical Engineering Department, Federal University of Espírito Santo (UFES), Fernando Ferrari Avenue, Vitória 29075-910, Brazil; [3]I3N & Physics Department, University of Aveiro, Aveiro 3810-193, Portugal.

*Correspondence: C Marques, E-mail: carlos.marques@ua.pt

Supplementary information for this paper is available at https://doi.org/10.29026/oea.2022.210098

Analytical model of bioinspired multifunctional photonic sensor

A central ring forms the sensor structure with a proof mass positioned over it and by eight bars fixed to the external side of the ring. The bars have angles of 45° to each other which provides symmetry for the structure in the direction of all bars. By measuring the deformation along the sensor structure at different points, it is possible to estimate the displacement of the proof mass and these variables may be related by a mathematical model.

When the sensor-proof mass is subjected to a displacement, the bars coupled to it tend to move. The movements of the end of the bars are parallel or perpendicular to their own axis, and for this reason, the complete system behavior can be modeled using dynamic equations of a group of equivalent mass-spring-damper systems on the endpoint for transversal and longitudinal directions. Assuming that the damping coefficient is the same for all the movement directions and obtaining the bar equivalent mass and stiffness, the Newton Second Law is applied on mass-spring-damper equivalent systems to obtain the differential equations of transversal and longitudinal movements of each bar endpoint. The elastic and damping forces over the bar are proportional to the relative displacement and relative velocity between the proof mass and the endpoint.

The bars do not have a direct connection to each other, so their models are uncoupled and can be analyzed separately. Due to the symmetry properties from the structure, the endpoints which are in the same direction and opposite sides have similar dynamic behavior when excited by the proof mass displacement and for this reason, the number of variables may be reduced by half.

Assuming a uniform bar under an axial concentrated load on its end, the equivalent mass and stiffness in the longitudinal direction are seen in Eqs. (S1) and (S2), respectively.

$$m_{\mathrm{a}} = \frac{\rho \cdot A \cdot L}{3}\ , \tag{S1}$$

$$k_{\mathrm{a}} = \frac{E \cdot A}{L}\ , \tag{S2}$$

where ρ is the density of the material of the bar, L is the bar length, A is the bar cross-section area and E is the material Young's modulus. A similar analysis can be done assuming a uniform cantilever beam under a perpendicular concentrated load on its end, the equivalent mass and stiffness in the transversal direction are seen in Eqs. (S3) and (S4), respectively.

$$m_{\mathrm{t}} = \frac{33 \cdot \rho \cdot A \cdot L}{140}\ , \tag{S3}$$

$$k_{\mathrm{t}} = \frac{3 \cdot E \cdot I}{L^3}\ , \tag{S4}$$

where I is the moment of inertia of the bar cross-section. Assuming the bar as uniform and full solid, the area and moment of inertia of the section are calculated as a function of the bar diameter.

Figure S1 presents the top view of the sensor structure for proof mass displacement on x-axis (Fig. S1(a)) and y-axis (Fig. S1(b)) and the respective reference systems used in which case. When the proof mass moves in x and y directions, the points which are on the diagonal positions have x' and y' displacement that results in movements projected in x and y.

Initially, considering the proof mass displacement only on the x-axis as input for the system, the points A1, A3, A5 and A7 have a movement only in the x-direction. The points A2, A4, A6, and A8 have components of displacement on the x'-axis (transversal for A2 and A6 and longitudinal for A4 and A8) and on y'-axis (longitudinal for A2 and A6 and transversal for A4 and A8).

The equations which relate the position, velocity, and acceleration on the bar extremity with the proof mass position and velocity on the x-axis may be written in matrix form (Eq. (S5)). Eq. (S6) to (S9) represents the mass, damping, stiffness, and excitation matrices respectively.

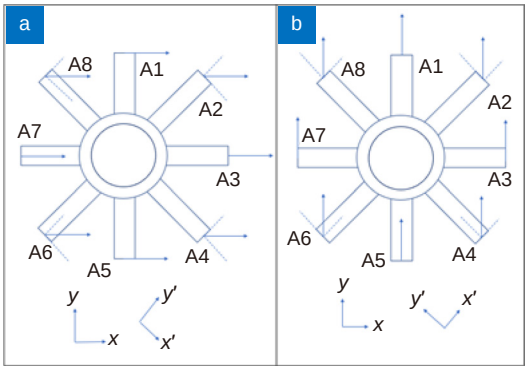

Fig. S1 | Top view of the sensor structure subjected to displacement in (**a**) *x*-axis and (**b**) *y*-axis.

$$[M_x]\cdot\begin{bmatrix}\ddot{x}_{15}\\ \ddot{x}_{37}\\ \ddot{x}'_{48}\\ \ddot{y}'_{48}\\ \ddot{x}'_{26}\\ \ddot{y}'_{26}\end{bmatrix}+[C_x]\cdot\begin{bmatrix}\dot{x}_{15}\\ \dot{x}_{37}\\ \dot{x}'_{48}\\ \dot{y}'_{48}\\ \dot{x}'_{26}\\ \dot{y}'_{26}\end{bmatrix}+[K_x]\cdot\begin{bmatrix}x_{15}\\ x_{37}\\ x'_{48}\\ y'_{48}\\ x'_{26}\\ y'_{26}\end{bmatrix}=[U_x]\cdot\begin{bmatrix}x_m\\ \dot{x}_m\end{bmatrix}, \tag{S5}$$

$$[M_x]=\begin{bmatrix}m_{\rm t}&0&0&0&0&0\\ 0&m_{\rm a}&0&0&0&0\\ 0&0&m_{\rm a}&0&0&0\\ 0&0&0&m_{\rm t}&0&0\\ 0&0&0&0&m_{\rm a}&0\\ 0&0&0&0&0&m_{\rm a}\end{bmatrix}, \tag{S6}$$

$$[C_x]=\begin{bmatrix}c&0&0&0&0&0\\ 0&c&0&0&0&0\\ 0&0&c&0&0&0\\ 0&0&0&c&0&0\\ 0&0&0&0&c&0\\ 0&0&0&0&0&c\end{bmatrix}, \tag{S7}$$

$$[K_x]=\begin{bmatrix}k_{\rm t}&0&0&0&0&0\\ 0&k_{\rm a}&0&0&0&0\\ 0&0&k_{\rm a}&0&0&0\\ 0&0&0&k_{\rm t}&0&0\\ 0&0&0&0&k_{\rm a}&0\\ 0&0&0&0&0&k_{\rm a}\end{bmatrix}, \tag{S8}$$

$$[U_x]=\begin{bmatrix}k_{\rm t}&c\\ k_{\rm a}&c\\ k_{\rm a}\cdot\cos45^\circ&c\cdot\cos45^\circ\\ k_{\rm t}\cdot\sin45^\circ&c\cdot\sin45^\circ\\ k_{\rm t}\cdot\sin45^\circ&c\cdot\sin45^\circ\\ k_{\rm a}\cdot\cos45^\circ&c\cdot\cos45^\circ\end{bmatrix}. \tag{S9}$$

The positions that are obtained for the points on the diagonal bars are on the x' and y' axis and can be projected on the Cartesian plane using Eqs. (S10) and (S11).

$$x=x'\cdot\cos45^\circ+y'\cdot\sin45^\circ, \tag{S10}$$

$$y=y'\cdot\cos45^\circ-x'\cdot\sin45^\circ. \tag{S11}$$

The same process is done for the case in which the entrance of the system is the proof mass displacement on the *y*-axis. The points A1, A3, A5, and A7 have a movement only in the *y*-direction. The points A2, A4, A6, and A8 have

components of displacement on the x'-axis (longitudinal for A2 and A6 and transversal for A4 and A8) and on the y'-axis (transversal for A2 and A6 and longitudinal for A4 and A8). The equations of motion of the extremity of the bar as a function of the proof mass position and velocity on y-axis are in matrix form in Eq. (S12). Eqs. (S13) to (S16) represents the mass, damping, stiffness, and excitation matrices respectively.

$$[M_y]\cdot\begin{bmatrix}\ddot{y}_{15}\\ \ddot{y}_{37}\\ \ddot{x}'_{48}\\ \ddot{y}'_{48}\\ \ddot{x}'_{26}\\ \ddot{y}'_{26}\end{bmatrix}+[C_y]\cdot\begin{bmatrix}\dot{y}_{15}\\ \dot{y}_{37}\\ \dot{x}'_{48}\\ \dot{y}'_{48}\\ \dot{x}'_{26}\\ \dot{y}'_{26}\end{bmatrix}+[K_y]\begin{bmatrix}y_{15}\\ y_{37}\\ x'_{48}\\ y'_{48}\\ x'_{26}\\ y'_{26}\end{bmatrix}=[U_y]\cdot\begin{bmatrix}y_m\\ \dot{y}_m\end{bmatrix}, \tag{S12}$$

$$[M_y]=\begin{bmatrix}m_{\mathrm{a}}&0&0&0&0&0\\0&m_{\mathrm{t}}&0&0&0&0\\0&0&m_{\mathrm{t}}&0&0&0\\0&0&0&m_{\mathrm{a}}&0&0\\0&0&0&0&m_{\mathrm{a}}&0\\0&0&0&0&0&m_{\mathrm{t}}\end{bmatrix}, \tag{S13}$$

$$[C_y]=\begin{bmatrix}c&0&0&0&0&0\\0&c&0&0&0&0\\0&0&c&0&0&0\\0&0&0&c&0&0\\0&0&0&0&c&0\\0&0&0&0&0&c\end{bmatrix}, \tag{S14}$$

$$[K_y]=\begin{bmatrix}k_{\mathrm{a}}&0&0&0&0&0\\0&k_{\mathrm{t}}&0&0&0&0\\0&0&k_{\mathrm{t}}&0&0&0\\0&0&0&k_{\mathrm{a}}&0&0\\0&0&0&0&k_{\mathrm{a}}&0\\0&0&0&0&0&k_{\mathrm{t}}\end{bmatrix}, \tag{S15}$$

$$[U_y]=\begin{bmatrix}k_{\mathrm{a}}&c\\ k_{\mathrm{t}}&c\\ k_{\mathrm{t}}\cdot\sin45^\circ&c\cdot\sin45^\circ\\ k_{\mathrm{a}}\cdot\cos45^\circ&c\cdot\cos45^\circ\\ k_{\mathrm{a}}\cdot\cos45^\circ&c\cdot\cos45^\circ\\ k_{\mathrm{t}}\cdot\sin45^\circ&c\cdot\sin45^\circ\end{bmatrix}. \tag{S16}$$

For this case, the positions that are obtained for the points on the diagonal bars are on the x' and y' axis and can be projected on the Cartesian plane using Eqs. (S17) and (S18).

$$x=x'\cdot\cos45^\circ+y'\cdot\sin45^\circ, \tag{S17}$$

$$y=x'\cdot\sin45^\circ-y'\cdot\cos45^\circ. \tag{S18}$$

The analysis for the proof mass displacement on the z-axis is simpler due to the symmetry of the sensor, which makes that all bars under the effect of the same excitation. Moreover, the motion equation of the bar endpoint on the z-axis is the same for points A1 to A8 since they have equal equivalent mass, damping, and stiffness in the transversal direction. Eq. (S19) provides the bars' endpoint position, velocity, and acceleration as a function of proof mass displacement on the z-axis.

$$m_{\mathrm{t}}\cdot\ddot{z}+c\cdot\dot{z}+k_{\mathrm{t}}\cdot z=k_{\mathrm{t}}\cdot z_{\mathrm{m}}+c\cdot\dot{z}_{\mathrm{m}}. \tag{S19}$$

If the inertia from the proof mass is significant in relation to the inertia of the bars, the acceleration of the mass has a direct influence on the movement of the bars. In this case, the movement of the proof mass is modified by an external force acting on it which is the new entrance of the system. For this approach, there is a coupling between all the bars

endpoint through the motion equations of the proof mass. The forces on the proof mass are the reaction of the elastic and damping forces from the bars and the external force. For the movements in the x and y direction, the structure symmetry makes the projections of the forces in the direction perpendicular to the movement of the mass cancel each other out.

Making the proper trigonometric simplifications, Eqs. (S20) and (S21) are the equations of motion on x and y directions with the same references presented in Figure 1 used for x' and y'.

$$\begin{aligned} m_{\mathrm{e}} \cdot \ddot{x}_{\mathrm{m}} + 8 \cdot c \cdot \dot{x}_{\mathrm{m}} + (4 \cdot k_{\mathrm{a}} + 4 \cdot k_{\mathrm{t}}) \cdot x_{\mathrm{m}} = {} & F_x + 2 \cdot k_{\mathrm{a}} \cdot x_{37} + 2 \cdot c \cdot \dot{x}_{37} + 2 \cdot k_{\mathrm{t}} \cdot x_{15} + 2 \cdot c \cdot \dot{x}_{15} + k_{\mathrm{a}} \cdot x'_{48} \\ & + c \cdot \dot{x}'_{48} + k_{\mathrm{a}} \cdot y'_{26} + c \cdot \dot{y}'_{26} + k_{\mathrm{t}} \cdot y'_{48} + c \cdot \dot{y}'_{48} + k_{\mathrm{t}} \cdot x'_{26} + c \cdot \dot{x}'_{26} \,, \end{aligned} \tag{S20}$$

$$\begin{aligned} m_{\mathrm{e}} \cdot \ddot{y}_{\mathrm{m}} + 8 \cdot c \cdot \dot{y}_{\mathrm{m}} + (4 \cdot k_{\mathrm{a}} + 4 \cdot k_{\mathrm{t}}) \cdot y_{\mathrm{m}} = {} & F_y + 2 \cdot k_{\mathrm{a}} \cdot y_{15} + 2 \cdot c \cdot \dot{y}_{15} + 2 \cdot k_{\mathrm{t}} \cdot y_{37} + 2 \cdot c \cdot \dot{y}_{37} + k_{\mathrm{a}} \cdot x'_{26} \\ & + c \cdot \dot{x}'_{26} + k_{\mathrm{a}} \cdot y'_{48} + c \cdot \dot{y}'_{48} + k_{\mathrm{t}} \cdot y'_{26} + c \cdot \dot{y}'_{26} + k_{\mathrm{t}} \cdot x'_{48} + c \cdot \dot{x}'_{48} \,. \end{aligned} \tag{S21}$$

For the z-direction, due to symmetry, the eight elastic and eight damping forces are equal, the dynamic model is simpler and can be seen in Eq. (S22).

$$m_{\mathrm{e}} \cdot \ddot{z}_{\mathrm{m}} + 8 \cdot c \cdot \dot{z}_{\mathrm{m}} + 8 \cdot k_{\mathrm{t}} \cdot z_{\mathrm{m}} = \boldsymbol{F}_z + 8 \cdot k_{\mathrm{t}} \cdot z + 8 \cdot c \cdot \dot{z} \,. \tag{S22}$$

In this case, m_{e} is the mass from the proof mass, and $\boldsymbol{F}_x$, $\boldsymbol{F}_y$, and $\boldsymbol{F}_z$ are the external forces in the x, y, and z-direction, respectively. It is possible to simulate the tridimensional spatial movement of the sensor structure as a function of an external load applied on it by relating all the obtained equations which model the motion of the sensor structure rigid bodies.